



PARAMETRIC STUDY OF PISTON RING FOR A SINGLE CYLINDER CI ENGINE

¹K S Kharadi,²Mehul N Patel

¹Lecturer in Mechanical Engineering, ²Research Scholar and Lecturer in Mechanical Engineering

^{1&2}Mechanical Engineering Department,

^{1&2}Government Polytechnic, Himmatnagar, Gujarat, India

Abstract : Tribology is the science of interacting surfaces in relative motion. It includes the study and application of the principles of friction, lubrication and wear. It is a high time to develop fuel efficient and environmental friendly compact automobile engines. In this development, tribology is crucial as this development needs incremental specific loads, speeds, temperatures and surface roughness for majority of frictional components and needs better lubricants. This inevitably results in a decrease in the thickness of the oil film between the interacting surfaces of these components and increases the significance of the two surfaces' surface profiles and topography in influencing tribological performance.

In internal combustion engine (ICE), majority of friction/wear occurs in bearings, piston pin, piston ring assembly (PRA), cam and follower, valve train, pumping losses etc. which are moving parts. From the literature, it is found that PRA contributes to 40-50% of total mechanical losses which accounts for 10-15% of total losses. Hence, it is tough to develop vehicles with greater efficiency, low fuel consumption and reduced environmental impact and that is where tribology comes into picture. Focusing on this, this work covers friction, lubrication and wears aspects encountered in the PRA of the ICE. Dry and Lubricated sliding wear behavior of grey cast iron piston ring has been studied using a TR-20-LE pin-on-disc apparatus at variety of load range and sliding velocity is used. For variety of crank angles, piston velocity, oil film thickness (OFT), hydrodynamic pressure and friction force, asperity contact pressure, contact load, asperity contact friction and total friction are achieved through theoretical analysis. On top of the same, parametric analysis is performed to analyze effect of engine speed, effect of lubricant viscosity, effect of ring tension, effect of surface roughness, and effect of ring width on friction force (FF) at different engine speeds and achieved results study has been undertaken to investigate the determinants of stock returns in Karachi Stock Exchange (KSE) using two assets pricing models the classical Capital Asset Pricing Model and Arbitrage Pricing Theory model. To test the CAPM market return is used and macroeconomic variables are used to test the APT. The macroeconomic variables include inflation, oil prices, interest rate and exchange rate. For the very purpose monthly time series data has been arranged from Jan 2010 to Dec 2014. The analytical framework contains.

Index Terms - Tribology, Piston ring assembly, Friction Force, Wear, Friction Coefficient.

I. INTRODUCTION

ICE are involved in routine life of humankind since starting of this decade. In ICE, PRA contributes almost 45-50% of total mechanical losses which is approximately 10 to 15% of the total fuel energy [1], [2], as is illustrated in Fig.1. The movement of piston and piston ring-pack in ICE are two largest contributors to engine mechanical losses.

Consequently, engine thermal efficiency will increase more with less friction in the piston and piston ring-pack than with the same reduction in other mechanical friction sources. Cutting down on piston and piston ring-pack friction also lowers the heat generated in the power cylinder, which lessens the thermal burden on the engine's cooling system [3]. In order to minimize wear and friction and have the least negative environmental impact possible, new power cylinder systems must be designed with a low amount of friction while preserving engine longevity [4].

The engine have wide range of operating conditions of speed, load, and temperature and it is tough to achieve effective lubrication of all moving engine components and that is where tribology comes into picture. Benefits achieved for engine by better tribological performance includes reduced fuel consumption, increased engine power output, reduced oil consumption, reduced harmful exhaust emissions, improved durability, reliability and engine life, and reduced maintenance requirements and longer service intervals.

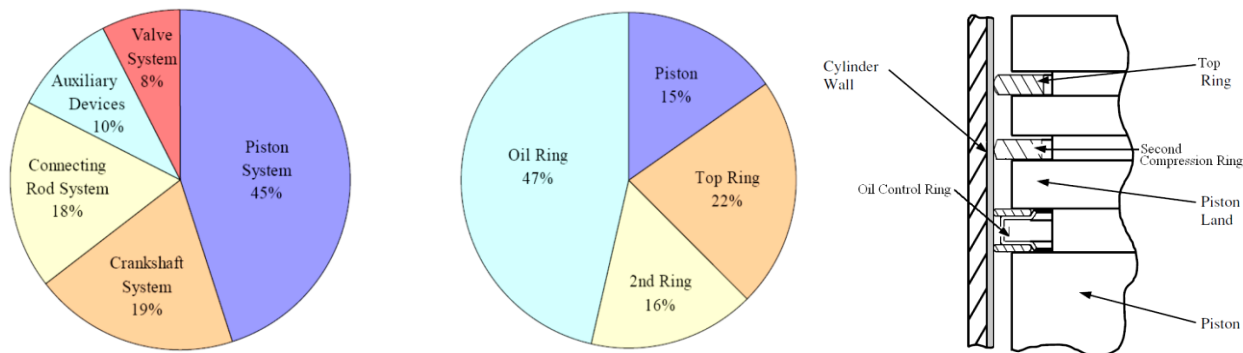


Fig.1 Left: Total fuel energy usage and engine mechanical losses [1], [2], Right: The piston ring pack [5]

Design-wise, piston rings are an essential part of ICEs and serve three primary purposes: first, they act as a seal to keep excessive amounts of combustion gases from leaving the chamber and into the crankcase; second, they keep lubricant from entering the chamber and being consumed during combustion; and third, they regulate piston temperature by transferring combustion heat from the piston to the cylinder liner, a function that is less significant in modern high output engines.

The piston ring-pack is a vital component in the efficient and reliable operation of an ICE. Lubrication is supplied to the piston ring-pack by flooding the cylinder liner with lubricant below the position of the oil control ring. A typical piston ring-pack in both gasoline and diesel engines contains three rings: an oil control ring, a second or scraper ring, and a top or compression ring. Design of each ring and its intended functions are described here. The top ring, located highest on the piston typically having a single barrel-shaped ring profile, prevents combustion gas blow-by. It's far from the oil control ring, leading to lubrication issues during strokes. High gas pressures and lack of lubrication make it susceptible to scuffing failure during engine cycles. The second scraper ring, a Napier style ring, is located between the oil control ring and top ring on the piston. It supports both the OCR ring and top ring by controlling lubricant supply, minimizing oil consumption, and preventing blow-by of combustion chamber gases. Due to greater oil supply and lower gas pressures, its contribution to ring-pack friction is typically small. The oil control ring (OCR) is the lowest ring on the piston, controlling lubricant flow to the top two rings. It consists of two or three components, including rails and a supporting spring. The OCR is the highest tension ring in the ring-pack, contributing half of total friction [1], [3], [6], [7].

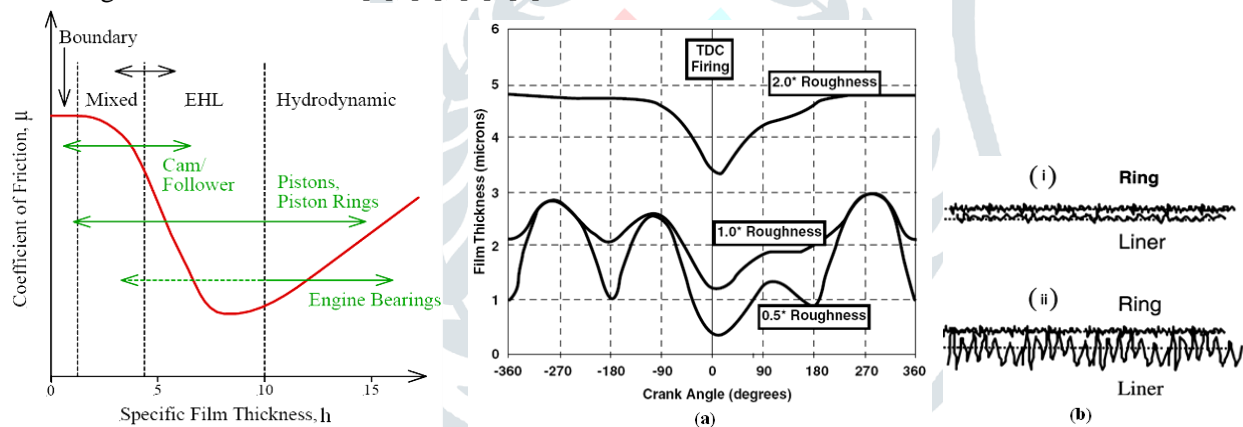


Fig.2 Left: Stribeck diagram [8], [9], Middle: OFT as a function of surface roughness, Left: Interaction of ring/liner asperities: (i) smooth liner surface, and (ii) rough liner surface [10].

With study of PRA, understanding of three modes of lubrication is important. Hydrodynamic lubrication occurs between a ring and liner when oil film thickness is large enough to prevent contact, typically during mid-stroke conditions with high sliding speeds. Mixed lubrication occurs when ring load is carried by hydrodynamic pressure in the lubricant film and rough surface contact, transitioning between boundary and hydrodynamic lubrication. Boundary lubrication occurs between a ring and liner when insufficient lubrication is available, with friction proportional to ring load, and occurs near the piston's stroke [11], [12]. With this Piston rings experience diverse lubrication conditions due to piston reciprocation, high gas pressures, and limited lubricant supply, ranging from hydrodynamic to boundary lubrication during an engine cycle. Fig. 2 represents different lubrication regimes in PRA by Stribeck diagram as Boundary lubrication, Mixed lubrication, Elastohydrodynamic lubrication and Hydrodynamic lubrication [8], [9]. Additives alter lubricant viscosity at different temperatures, affecting friction based on lubrication, surface roughness, ring geometry, and asperity contacts. The predicted oil film thickness (OFT) under the face of the top compression ring as a function of crank angle for various cases of liner roughness is shown in Figure 3. The OFT is defined as the distance between the mean height of the asperities on the surface.

The oil film thickness changes with liner roughness, with thicker oil films formed during high-pressure periods. Lower surface roughness results in more variations in the predicted OFT. The minimum OFT for fluid film lubrication depends on surface finish, elastic modulus, thermal distortion, and contaminants' clearance space size. Liner surfaces with a roughness of 0.8-0.9 μm typically have a similar minimum OFT [1], [12]. Wear is a systems response where

wear rate of a material can vary from 10^{-3} to 10^{-10} mm³/Nm depending on contact conditions, such as the counterpart material, contact pressure, sliding velocity, contact shape, suspension stiffness, environment and the lubricant. The wear rate changes through the repeated contact process under constant load and velocity. It is generally high in an initial unsteady state and relatively lower in the later steady one [4], [13].

II. LITERATURE REVIEW

Tribology, a scientific study of friction, has a long history, with basic laws of friction developed by Leonardo da Vinci in the 15th century. Amonton in 1699 proposed that surfaces were covered by small spheres, and friction coefficient was determined by contact angle. Osborne Reynolds' 1886 paper on hydrodynamic lubrication led to further research, resulting in high-sophisticated journal bearing designs. Tribology is still imperfect and subject to controversy, hindering information diffusion to technologists. Table 1 represents literature survey towards the work.

Table 1: Literature survey

Researcher's work	Details of the work
[14]	Researchers represents a model based on stochastic theory simulates the impact of one-dimensional roughness on piston ring surface lubrication and friction, showing a higher FF and power loss in rough surfaces.
[15]	Researchers studied one-dimensional analysis of lubrication between piston rings and cylinder walls reveals that higher sliding speed promotes hydrodynamic lubrication, increasing power loss. Higher ring tension leads to higher loading, decreasing film thickness and power loss. Lower crown height increases minimum film thickness around dead centers, while larger ring width promotes hydrodynamic lubrication and decreases boundary lubrication.
[16]	This study investigates the impact of lubricant starvation on piston ring lubrication, focusing on a complete ring pack. It uses a one-dimensional piston-ring analysis and a computer code to solve the starved lubrication problem. The findings show that lubricant starvation significantly reduces the minimum film thickness of compression rings in mid-stroke, and in fully flooded conditions, the minimum oil film thickness increases with ring width.
[17]	Researchers studied the use of multi grade oil in engine lubrication to minimize viscosity-temperature effects. They developed a theoretical model predicting thinner oil films due to the introduction of multi grade oil in the hydrodynamic zone and larger piston travel distance near the TDC region. The study found that multi grade oil reduces FF due to shear thinning, but increases wear near the TDC region. The elasticity effect of multi grade oil contributes to separation and low friction.
[17]	Researchers studied the use of multigrade oil in engine lubrication to minimize viscosity-temperature effects. They developed a theoretical model predicting thinner oil films due to the introduction of multigrade oil in the hydrodynamic zone and larger piston travel distance near the TDC region. The study found that multigrade oil reduces FF due to shear thinning, but increases wear near the TDC region.
[18]	Researchers studied hydrodynamic model reveals that reducing piston ring friction and tension, and using two-ring packages, can improve fuel economy. However, these measures can also lead to excessive wear and increased oil consumption. Tateishi found that reducing friction can reduce fuel consumption by several percent, while tension reduction and two-ring packages are effective. TiN or Cr2N PVD can also improve piston ring wear and corrosion resistance.
[19]	Researchers developed a two-dimensional elastohydrodynamic cavitation algorithm for piston ring lubrication, examining circumferential flow effects. Results showed that hydrodynamic pressure decreases with increasing film thickness in the circumferential direction, and pressure reformation effect cannot be ignored when piston ring moves away from top dead center.
[20]	Researchers conducted a two-dimensional analysis of piston ring lubrication, considering elastic deflection, EHL, and cavitation effects. Results showed that piston ring deflection reduces gap caused by minimum film thickness uniformly in the circumferential direction. Oil film thickness around TDC is thicker in elliptical cylinders.
[21]	Researchers developed a finite difference solution for the two-dimensional Reynolds equation and a flow-continuity algorithm for 'starved' lubrication, which evaluates piston rings' tribological performance in circular and distorted bores. Factors like bore distortion, ring conformability, and axial motion are considered. Circular bores have larger friction, leading to higher power loss. Bore distortion is advantageous for energy savings but undesirable for oil consumption.
[22]	Researchers highlight the significant contribution of power cylinder friction to engine losses, comparing it to total energy production and overall mechanical friction. Fired engines have almost equal power cylinder friction to motored engines, with higher friction around TDC and less in low pressure regions. Lower viscosity oils can reduce friction, but formulation and power cylinder design changes are necessary to minimize wear.
[23]	Researchers used an axi-symmetric, hydrodynamic, mixed lubrication model to simulate frictional performance of piston ring and cylinder liner contact. They predicted FF, surface flow factors, roughness, and metal-to-metal contact loading. The model showed hydrodynamic lubrication in most of the stroke, but increased friction coefficient near dead centers due to mixed lubrication. This model could aid in designing new piston ring and cylinder liners.
[24]	Researchers used a bench friction test system to verify an analytical mixed lubrication model for piston ring and liner contact. They investigated the effects of running speed, normal load, contact temperature, and surface roughness on friction coefficient in cast-iron cylinder bores. Results showed temperature, surface roughness, and running speed are important parameters.
[5]	The study explains the importance of oil volume and residence time in high-temperature environments for lubricating piston rings. They present a model that includes various mechanisms and evaluates their influence on piston ring pack lubrication in automotive gasoline engines. The study suggests that additional mechanisms are needed for improved oil transport predictions, including oil flow around the piston assembly and at the ring/cylinder interface.
[25]	Researchers conducted tests on piston ring and cylinder liner materials' friction and wear behavior in realistic engine oils. They developed new standard test methods and tested a range of lubricants, including Jet A aviation fuel, mineral oil, and engine-aged 15W40 heavy duty oil. The tests showed boundary lubrication behavior at 1000C, with differences among lubricants detected.
[26]	Researcher study explains that wear occurs due to direct contact between mating surfaces under mixed or boundary lubrication. They propose a realistic liner/ring wear simulation based on surface asperity contact force. Higher cylinder

	wall temperatures lead to smaller oil film thickness and larger wear, while viscous shearing friction decreases and asperity contact friction increases. Higher surface roughness leads to higher friction and wear.
[27]	The study examined the impact of lubricant viscosity on oil film thickness and temperature in a diesel engine piston ring. They found that as ring sliding speed increases, oil film thickness thickens and inflow increases, causing a decrease in oil film temperature and lower liner temperature. The study also found that oil film thicknesses decrease with lower viscosity.
[28]	Researchers conducted a bench-test on six bore finishes of combustion engines against PVD-coated rings. Results showed that lubricant doping with hard particles and higher load and speed accelerate wear rate. Smoother surfaces showed lower ring and bore wear, with smoother surfaces entering the hydrodynamic regime earlier. Surface finish effect was not significant.
[29]	The study found that anticipated emission legislation and reduced fuel consumption are key factors in engine development. They simulated and experimentally tested the effects of surface topography and texture direction on oil film thickness and friction. Results showed low wear with glide-honed smooth liner surfaces, and average friction can be reduced with smoother surfaces.

From the above literature review (LR) it is observed that, the fuel energy distributed in various component of an ICE is about 30% in Exhaust, 30% in Cylinder Cooling, 15% in Mechanical Losses and 25% in Brake Power. It is also observed that the Mechanical losses distribution in ICE is 10% in Valve Train, 20% in Pumping Losses, 25% in Bearing and 45% in Piston Assembly. Further, it is observed that the mechanical losses distributed in piston ring assembly is 15% in piston, 22% in top ring, 16% in second ring and 47% in oil control ring. The friction losses in PRA are totally depends on the minimum oil film thickness, hydrodynamic pressure in the oil film thickness, surface roughness of the both piston ring and cylinder liner material.

The objectives derived from LR were to study the PRA performance of an ICE and inter ring pressure for measuring the oil film thickness and friction between piston ring and cylinder liner, to study the minimum oil film thickness between the piston ring and cylinder liner with the FF measurement methods of the PRA and to solve the Reynolds equation of the lubrication by using suitable numerical method and computer software. This is to identify and study effects of parameters such as engine speed, different types of lubricants, surface roughness of the piston ring and cylinder liner, piston ring geometry, ring tension on friction power loss in the engine.

III. THE REYNOLDS' HYDRODYNAMIC LUBRICATION AND RELATED MATHEMATICAL TERMS

Reynolds' theory explains lubrication by creating a viscous liquid film between moving surfaces, requiring sufficient velocity for film generation. This equation, derived by Reynolds, is commonly used to express hydrodynamic lubrication. This is adopted with general common assumptions for the equation. Considering a small element under the action of the viscous shear stresses and the fluid pressure is really the starting point of Reynolds' equation. In the process of derivation, it can be seen that the shear stress is replaced by the viscosity and the rate of shear where Newton's law of viscous flow comes into picture. Consider then the problem of the equilibrium of a small element of lubricant as shown in figure 3.

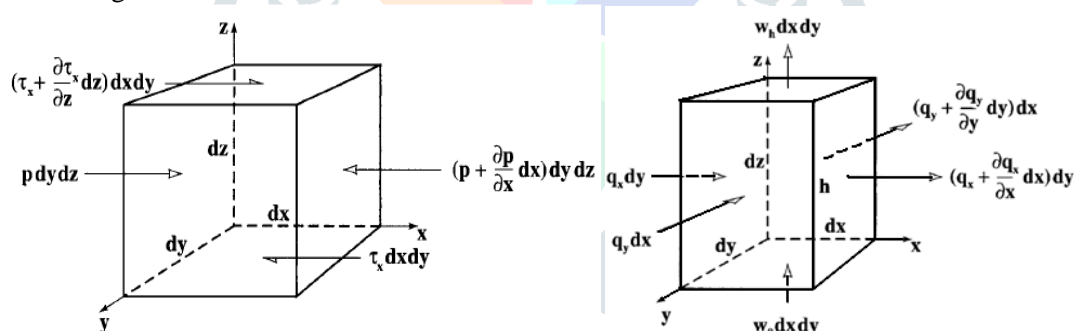


Fig. 3 Left: Equilibrium of an element fluid from a hydrodynamic film [30], Right: Continuity of flow in a column [30]

Where, p is the pressure, x is the shear stress acting in the 'x' direction. The three separate terms in any of the velocity equations (3.11) and (3.12) represent the velocity profiles across the fluid film. The principle of continuity of flow requires that the influx of a liquid must equal its efflux from a control volume under steady conditions. The simplified full Reynolds equation in three dimensions is as below.

$$\frac{\partial}{\partial x} \left(\frac{h^3}{12\eta} \frac{\partial p}{\partial x} \right) + \frac{\partial}{\partial y} \left(\frac{h^3}{12\eta} \frac{\partial p}{\partial y} \right) = U \frac{dh}{dx} + V \frac{dh}{dy} + 12(w_h - w_0)$$

Reynolds equation for squeeze films: The Reynolds equation with the squeeze term is in the form,

$$\frac{\partial}{\partial x} \left(\frac{h^3}{\eta} \frac{\partial p}{\partial x} \right) + \frac{\partial}{\partial y} \left(\frac{h^3}{\eta} \frac{\partial p}{\partial y} \right) = 6U \frac{dh}{dx} + 12 \frac{dh}{dt}$$

This is helpful in prediction of bearing parameters such as pressure distribution, load capacity; FF, coefficient of friction and oil flow are obtained by simple integration. Lubricant flow is extremely important to the operation of a bearing since enough oil must be supplied to the hydrodynamic contact to prevent starvation and consequent failure. The flow formulae are expressed in terms of bearing parameters and the lubricant flow can also be optimized. Numerical analysis of Reynolds equation can be done by the Finite Difference Methods where analytical solution of partial differential equations of first or second order that involves closed form expressions that provide the variation

of the flow field variables continuously throath the domain. This is in contrast to numerical solutions where they provide answers only at discrete points in the geometric domain and can be in one dimension or in two dimensions. However, in the actual Reynolds equation the oil film thickness h , term is included inside the second derivative. In the present work, squeeze film velocity is not considered. The output of equations in the form of matrix can be solved using MATLAB 2007a which is used in analysis. MATLAB is a software package for high-performance numerical computation and visualization. It provides an interactive environment with hundreds of built-in functions for technical computation, graphics, and animation. Best of all, it provides easy extensibility with its own high-level programming language. The name MATLAB stands for MATrix LABORatory. This proportion is not covered under this research.

IV. EXPERIMENTAL INVESTIGATION AND PERFORMANCE

Wear is a systems response where rate can vary from 10^{-3} to 10^{-10} mm³/Nm depending on contact conditions, such as the counterpart material, contact pressure, sliding velocity, contact shape, suspension stiffness, environment and the lubricant. The wear rate changes due to repeated contact under constant load and velocity, typically high in an initial unsteady state and lower in a steady state. In this experiment, Dry and Lubricated sliding wear behavior of grey cast iron piston ring has been studied using a TR-20-LE pin-on-disc apparatus at load range of 5N to 200N and sliding velocity of 0.5m/s to 10 m/s. Coefficient of friction and FF of the conventional and chrome coated piston ring has been compared here.

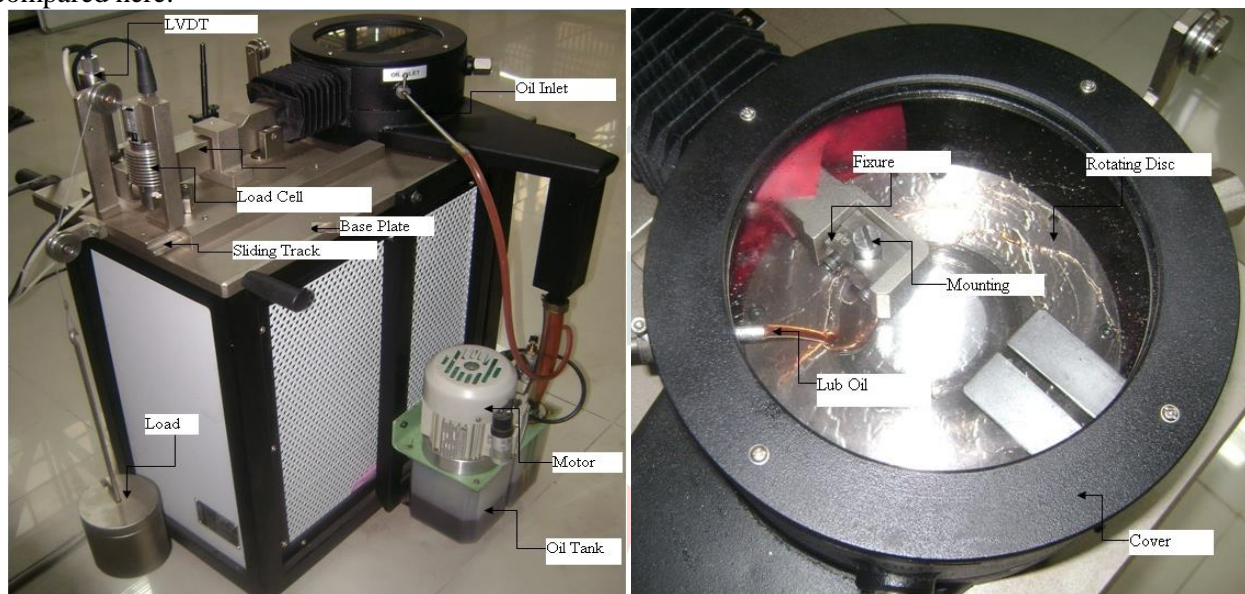


Fig. 4 Left: Test Rig for Friction and Wear Monitoring & Right: Mounting of Ring Specimen on Rotating Disc

Test Rig: The TR-20-LE Pin on disc wear testing machine is a significant advancement in simplicity, convenience, and accuracy in measuring wear and frictional force. It can apply up to 20 kg and is suitable for dry and lubricated test conditions. The machine monitors frictional force and wear using electronic sensors and records parameters. It determines wear and coefficient of friction on metals under sliding contact and evaluates material rate and ranking. Table 2 is representing specifications of test rig.

Table 2: Rotating Disc Test Rig Technical Specification

Details	Description	Remarks
Rotating Disc	Dia 165* 8mm Thick	Material- En-31 hardened to 62HRC
Disc Speed	200 to 2000 rpm	Infinitely variable in steps of 1 rpm
Normal Load	5 to 200 N	
Frictional Force	0 to 200 N	
Wear	± 2 mm	
Wear Track diameter	50 to 100 mm	
Sliding Speed	0.5 to 10 m/sec	
Timer	Max. 99 hrs, 59 min, 59 sec	

Test rig contains rotating disc, made up of hard material, which is rotates at constant speed, wear track diameter at which the point load acting from center, by adjusting track diameter we vary the **sliding distance**. Here, we adjust the track diameter upto 70 mm for the experiment for all the case. **Fig. 5 Wear Track Diameter for setting Sliding distance**

It also contains **data logger** to records all the data as a sample rate as per required, track diameter, test duration, frictional force, wear in micron, sliding speed and also



displaying the frictional force (N), wear (micrometer), speed (rpm) and time (second), and directly transmits all the relevant values to the computer software Windcum 2008 were installed already. Attached LVDT measure the wear depth with range of ± 2 mm and transmit the data to the Data logger. It is very sensitive, so it is require much trained person to operate. The **piezoelectric load sensor** is mountain on top of the test rig which is transmits the wear depth of the test specimen in terms of micron to the data logger and displayed on the computer software directly. The **motor and oil pump** are used to provide sufficient flow rate of lubricant oil in lubricated test.

Test specimen of Piston Ring and test procedure:

Figure 6 represents mounting of the piston ring on the steel round bar. For the fixing the segments of piston ring in solid steel bar having diameter of 12 mm. A groove is made on the top surface by milling at our central workshop for proper fixing arrangement. **Fig. 6 Piston Ring Piece and its Mounting.** The mounting of test specimen is very difficult during testing because of machine vibration, in this test the care has been taken for it by applying araldite. In tests, dry sliding wear tests were conducted on a pin-on-disc apparatus, applying different loads to a piston ring piece against a hardened steel disc. The tests were conducted for a total sliding distance of 6594 meters, with weight measurements, polishing, cleaning, and drying. The FF was continuously monitored to determine the coefficient of friction, and the volumetric wear coefficient was calculated from weight loss measurements.



Investigation through experimentations: (Viscosity Measurement): Study of Viscosity with Redwood Viscometer: A viscometer is a vertical cylinder filled with liquid, heated by an electric heater, to determine its viscosity, which is maintained in a water bath. Then orifice is opened and the time required to pass 50ml. of oil is noted. In case of redwood viscometer the kinematic viscosity (μ) of liquid and the time (t) required to pass 50ml. of liquid are correlated by the expression. Equation is: $\mu=0.26t-171/t$, where, μ = Kinematic viscosity in centistokes and t= Time in seconds to collect 50ml. of oil. Three samples were taken namely **Castrol (20W40 Diesel Oil), Lal Ghoda (20W40 Diesel Oil) and Castrol CRB+ (20W40 Diesel Oil).** Graphs for viscosity v/s temperature are obtained.

Results of the experiments:

A. Results of the Kinematic Viscosity of Lubricating Oils Kinematic Viscosity of Castrol (20W40 Diesel Oil)

Sr. No.	Temperature (oC)	Time (sec)	Kinematic Viscosity (Cst)
1	40	377	97.6
2	50	238	61.2
3	60	173	44.0
4	70	161	40.8
5	80	98	23.7
6	90	85	20.1
7	100	70	15.8

Kinematic Viscosity of Lal Ghoda (20W40 Diesel Oil)

Sr. No	Temperature (oC)	Time (sec)	Kinematic Viscosity (Cst)
1	40	386	99.92
2	50	281	72.45
3	60	223	57.21
4	70	154	38.93
5	80	130	32.48
6	90	82	19.23
7	100	70	15.76

Kinematic Viscosity of CRB+ (20W40 Diesel Oil)

Sr. No	Temperature (oC)	Time (sec)	Kinematic Viscosity (Cst)
1	40	368	95.22
2	50	308	79.52
3	60	214	54.84
4	70	139	34.91
5	80	100	24.29
6	90	81	18.95
7	100	74	16.93

B. Results of the Surface Roughness of the Piston Ring and Cylinder Liner
Surface Roughness for Cylinder Liner

Sr. No.	Cylinder Liner, Ra value (micron)	Average Value (micron)
1.	0.38	0.44
2.	0.53	
3.	0.48	
4.	0.31	
5.	0.46	
6.	0.48	

Values of Surface Roughness for Piston Ring

Sr. No.	Ring	Conventional Ring Ra Values (micron)	Coating Ring (Chrome) Ra Values (micron)
1.	Top Ring	0.86	0.86
		0.63	0.63
		0.54	0.54
2.	Second Ring	0.73	0.59
		0.79	0.64
		0.64	0.57
3.	Third Ring	0.88	0.48
		0.77	0.65
		0.71	0.58

C. Results of the Ring Tension

Values of Ring Tension for Piston Ring

Sr. No.	Conventional Ring		Coating Ring (Hard Chrome)	
	(kg)	(N)	(kg)	(N)
1.	21	210	22	220
2.	18	180	19	190
3.	18	180	19	190

In line to this, a wear resistance coating of Piston Ring with hard chrome by electroplating was done with the aim to improve surface properties of a bulk material. Coating improves appearance, adhesion, wet ability, corrosion resistance, wear resistance, scratch resistance, etc. Setup of the same is not shown here. Coating can give prolonged protection against wear. Abrasive wear, adhesive wear and fretting are often reduced by wear resistant coatings.

Graphical representation is as below:

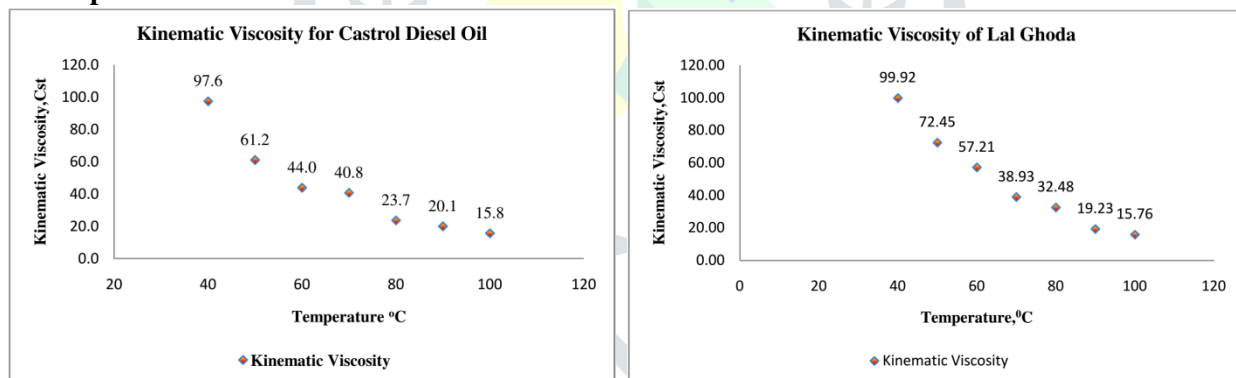
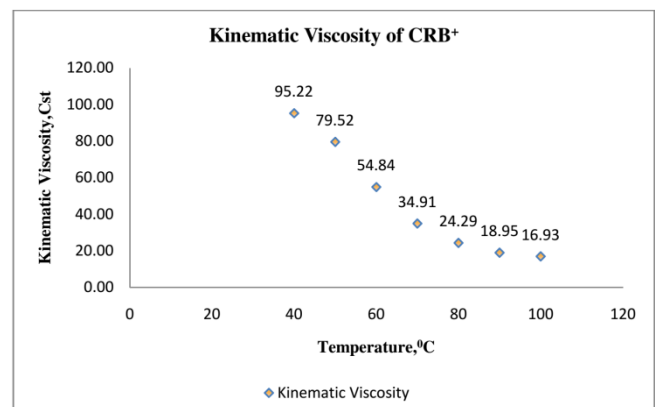


Fig.7 Kinematic Viscosity v/s Temperature for Different Oils

Surface Roughness Test: Figure 8 represents surface roughness test for cylinder liner and piston ring respectively. It was measured at six and three different points around the radial locations of every 60° and takes the average of them for calculations. Surface roughness for all the ring as a Top piston ring and compression rings are measured in same way. **Tension Measurement of Piston Ring Tension** for both piston ring top ring and compression ring is done as shown. This ring tension tester gives the value of ring tension in the terms of kg. **A portable surface roughness tester (TR100) was used for measuring surface texture conforming to traceable standards as it is easy in handling. Fig.8 (Right) Surface Roughness Test.**



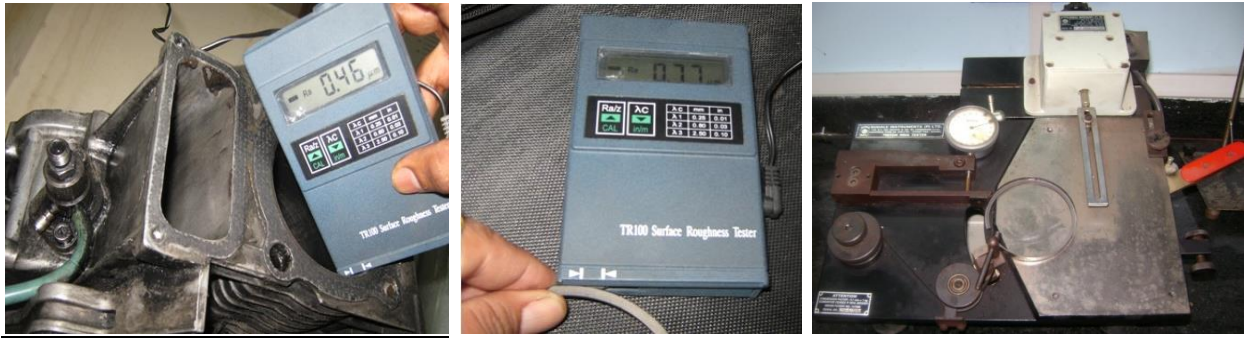


Fig. 8 Surface Roughness Test for Cylinder Liner and Piston Ring and Piston Ring Tension Tester

SPECIFICATIONS OF ENGINE UNDER STUDY

For modeling and simulation of friction models the Lombardini 400 CC Air cooled Diesel Engine is used. The engine specifications are as follows.

Table 4.1.Engine Specifications

Engine	Lombardini 15LD 400
kw	4.7 @ 3000
Type	4-stroke
RPM	3000
Number of Cylinders	1
Capacity	400 cc
Cooling	Air Cooled
Operational Parameters	
Bore (D)	82 mm
Stroke (S)	76 mm
Connecting rod length (L)	122 mm
Composite Roughness (σ)	0.8021
Viscosity (μ)	$54.84 \times 10^{-6} \text{ m}^2/\text{sec}$
Speed (N)	1000 RPM
Friction coefficient	0.15
First compression ring	
Axial width	2 mm
Radial width	3 mm
Tension	210 N
Second compression ring	
Axial width	2 mm
Radial width	3 mm
Tension	190 N

SIMULATION OF SOME FRICTION MODEL

Engine Kinematics: In an analysis of the lubrication of piston rings it is necessary to determine the velocity for both piston and piston ring which are function of crank angle. The Piston position and Piston velocity at the different crank angle is given by following equations [29].

$$S = R \left[1 - \cos \theta + \frac{1}{2} \left(\frac{R}{l} \right) \sin^2 \theta \right] \dots (3)$$

$$U = R \omega \left[\sin \theta + \frac{1}{2} \left(\frac{R}{l} \right) \sin 2\theta \right] \dots (4)$$

V. ANALYSIS AND RESULTS

Based on the selected engine, experimentations were done for variety of crank angles and piston velocity, oil film thickness, hydrodynamic FF, hydrodynamic pressure, contact pressure, contact load, asperity FF and total frictional force were obtained theoretically and parametrically. For **Kinematics of Piston-Connecting Rod-Crank Mechanism,**

Sample Calculations:

⇒ Piston Position:

$$S = R \left[1 - \cos \theta + \frac{1}{2} \left(\frac{R}{l} \right) \sin^2 \theta \right]$$

$$S = 0.038 \left[1 - \cos 75 + \frac{1}{2} \left(\frac{0.041}{0.122} \right) \sin^2 75 \right]$$

$$S = 0.03369 \text{ m}$$

⇒ Piston Velocity:

$$U = R \omega \left[\sin \theta + \frac{1}{2} \left(\frac{R}{l} \right) \sin 2\theta \right]$$

$$U = 0.038 \times 104.72 \left[\sin 75 + \frac{1}{2} \left(\frac{0.041}{0.122} \right) \sin 150 \right]$$

$$U = 4.1536 \text{ m/sec}$$

➤ Minimum oil film thickness:

$$h = A + B |\sin(\theta)|$$

$$h = 2 + 10 |\sin(75)|$$

$$h = 11.6593 \text{ micron}$$

➤ Hydrodynamic Pressure

$$p = \frac{6U\eta B}{Kh_0} \left[-\frac{1}{h} + \frac{h_0(K+1)}{h^2(K+2)} + \frac{1}{h_0(K+2)} \right]$$

$$p = \frac{6 \times 4.1536 \times 54 \times 10^{-6} \times 0.002}{1.2 \times 5 \times 10^{-6}} \left[-\frac{1}{2.872} + \frac{5 \times 10^{-5} (1.2+1)}{2.872^2 (1.2+2)} + \frac{1}{5 \times 10^{-6} (1.2+2)} \right]$$

$$p = 28.474 \times 10^3 \text{ pa}$$

➤ Load capacity

$$\frac{W}{L} = \frac{6U\eta B^2}{K^2 h_0^2} \left(-\ln(K+1) + \frac{2K}{K+2} \right)$$

$$\frac{W}{L} = \frac{6 \times 4.1536 \times 54.84 \times 10^{-6} \times 0.002^2}{1.2^2 (5 \times 10^{-6})^2} \left(-\ln(1.2+1) + \frac{2 \times 1.2}{1.2+2} \right)$$

$$W = -5.841 \text{ N}$$

➤ Hydrodynamic FF

$$\frac{F}{L} = \frac{U\eta B}{h_0} \left(\frac{6}{K+2} - \frac{4 \ln(K+1)}{K} \right)$$

$$\frac{F}{L} = \frac{4.1536 \times 54.84 \times 10^{-6} \times 0.002}{5 \times 10^{-6}} \left(\frac{6}{1.2+2} - \frac{4 \ln(1.2+1)}{1.2} \right)$$

$$F = -4.4399 \text{ N}$$

Samuel Eilon and et. al. Model

➤ Piston friction:

$$F_p = A_p \eta U \left(\frac{4}{h_p} + \frac{3c}{h_p^2} \right)$$

$$F_p = 0.017538 \times 54.84 \times 10^{-6} \times 4.1536 \left(\frac{4}{50 \times 10^{-6}} + \frac{3 \times (-0.1047 \times 10^{-3})}{(50 \times 10^{-5})^2} \right)$$

$$F_p = 0.2374597 \text{ N}$$

➤ Ring Friction:

$$F_r = \pi D \eta U \left[\frac{3cb}{2h_r^2 \left(1 + \frac{b^2}{2Rh_r} \right)} + \left(4 + \frac{3c}{2h_r} \right) \frac{\sqrt{2Rh_r}}{h_r} \tan^{-1} \frac{b}{\sqrt{2Rh_r}} \right]$$

$$F_r = \pi \times 0.082 \times 54.84 \times 10^{-6} \times 4.1536 \times \left[\frac{3(-0.1047 \times 10^{-3}) \times 0.001}{2(5 \times 10^{-6})^2 \left(1 + \frac{0.001^2}{2 \times 0.06 \times 5 \times 10^{-6}} \right)} + \left(4 + \frac{3 \times (-0.1047 \times 10^{-3})}{2 \times 5 \times 10^{-6}} \right) \frac{\sqrt{2 \times 0.06 \times 5 \times 10^{-5}}}{5 \times 10^{-6}} \tan^{-1} \frac{0.001}{\sqrt{2 \times 5 \times 10^{-6} \times 0.06}} \right]$$

$$F_r = -0.03299 \text{ N}$$

Y Tateishi Model➤ **Piston Ring Friction:**

$$F_r = c \left[\mu U \left(\frac{200W_{RT}}{D} \right) \right]^{0.5}$$

$$F_r = 1.1385 \times \left[54.84 \times 10^{-6} \times 4.1536 \left(\frac{200 \times 210}{0.082} \right) \right]^{0.5}$$

$$F_r = 12.2974 \text{ N}$$

M. Hoshi Model➤ **Piston friction:**

$$F_p = 0.6 D r^{0.5} N^{0.5} \mu^{0.5} \left| \sin\theta + \frac{\rho}{2} \sin 2\theta \right|^{0.5}$$

$$\times \left[\begin{array}{l} \sum \{B(P_x + P_r)\}^{0.5} + 0.20 D^{0.5} \delta^{0.5} \rho^{0.5} \\ \times \left| \sin\theta \left[P + 0.0014 \left(\frac{r}{D^2} \right) W N^2 \left\{ \cos\theta + \frac{\rho}{2} \cos 2\theta \right\} \right] \right|^{0.5} \end{array} \right]$$

$$F_p = 0.6 \times 0.082 (54.84 \times 10^{-6})^{0.5} 1000^{0.5} (54.84 \times 10^{-6})^{0.5} \times$$

$$\left| \sin 75 + \frac{0.311}{2} \sin 150 \right|^{0.5} \times$$

$$\left[\begin{array}{l} \sum \{0.002(P_x + P_r)\}^{0.5} + 0.20 \times 0.082^{0.5} 0.039^{0.5} 0.311^{0.5} \\ \times \left| \sin 5 \left[P + 0.0014 \left(\frac{0.038}{0.082^2} \right) 0.426 \times 1000^2 \left\{ \cos 75 + \frac{0.311}{2} \cos 150 \right\} \right] \right|^{0.5} \end{array} \right]$$

$$F_p = 1.306 \times 10^{-4} \text{ N}$$

By solving above equations for variety of crank angles, results obtained are represented as graphs below.

Theoretical Analysis of Parameters

Piston velocity: To study the lubrication of piston ring it is necessary to know the velocity of piston with every crank angle. Figure 9 demonstrates piston velocity variation with crank angle, increasing up to 90 degrees. It decreases after 90 degrees due to piston reciprocating motion, peaking at mid-stroke and decreasing at dead centers.

Minimum oil film thickness (OFT): Figure 9 represents minimum OFT for three different lubrication modes. The minimum oil film thickness value for Hydrodynamic, Mixed and Boundary Lubrications are 2, 1 and 0.5 respectively as per reported in literature [2]. The OFT is very significant parameter to involve in piston ring FF. OFT at the mid stroke of the engine cycle is most of large because of at that pure hydrodynamic lubrication occurred and at the dead centers, it is very less due to low piston velocity and oil squeeze effect. **Hydrodynamic Pressure:** Hydrodynamic pressure increases with increases the piston velocity with crank angle and nature of curved is found in sine wave. Figure 10 represents the maximum pressure of oil film thickness is about 2.85×10^4 Pa. **Hydrodynamic FF:** The hydrodynamic FF depends upon the engine speed and lubricant viscosity and is maximum at the mid stroke of the engine cycle. Figure 10 represent it about 4.5N.

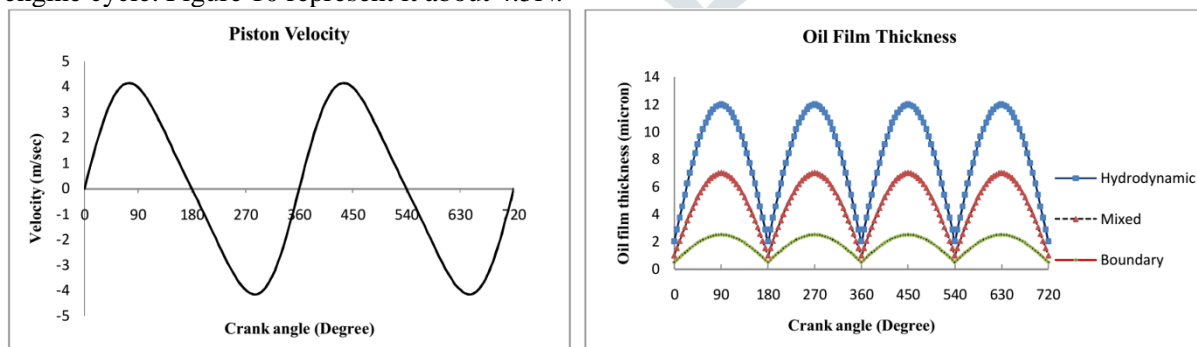


Fig. 9 Piston Velocity v/s Crank Angle and Oil Film Thickness v/s Crank angle.

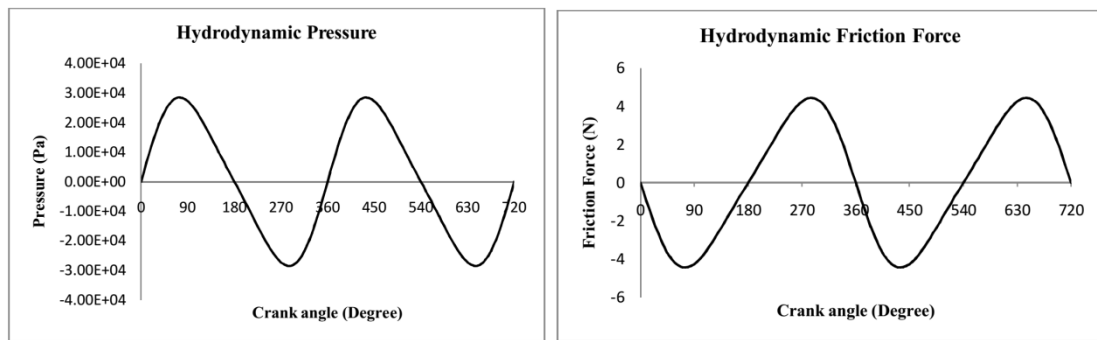


Fig. 10 Hydrodynamic Pressure and Friction v/s Crank Angle

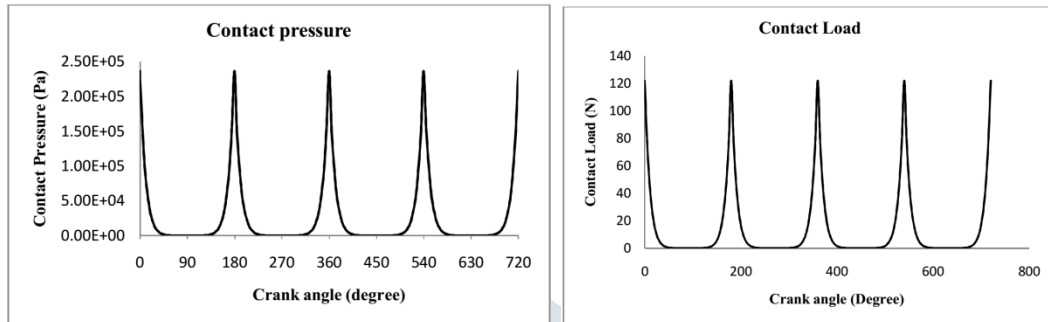


Fig. 11 Asperity Contact Pressure and Contact Load v/s Crank Angle

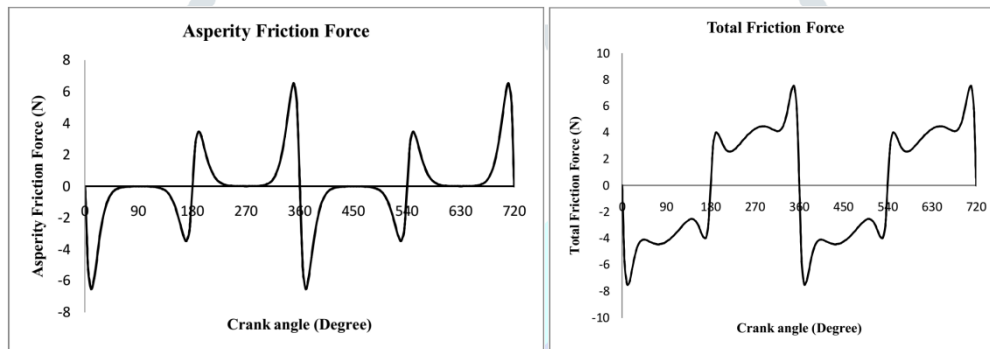


Fig. 12 Asperity Friction Force and Total Friction Force v/s Crank Angle

Contact Pressure: Asperity FF calculation involves contact pressure between surfaces. Oil film thickness generates higher contact pressure at Top dead center (TDC) and Bottom dead center (BDC), with lower pressure at the center due to hydrodynamic lubrication. The contact load is also higher at the TDC and BDC and lower at the middle of the stroke. The contact load depends upon the contact pressure as well as the contact surface area. **Asperity FF:** Asperity FF significantly depends upon the composite surface roughness of both cylinder liner and piston ring material. The Asperity FF is maximum at the TDC and BDC but lower at the middle stroke. It is observed that the asperity FF is maximum at dead centers about 6.5 N. **Total FF:** The total FF is depends upon the both hydrodynamic as well as asperity friction force. The nature of above curve is well similar with published work. The total FF is maximum is about 7.7 N at dead centers.

Parametric Analysis

Effect of Engine Speed on FF: It is observed that the hydrodynamic FF is increases with increases the engine speed and attain maximum value in case of 3000 rpm. Generally, it is concluded as the engine speed increases, the FF is also increased (figure 13). **Effect of Lubricant Viscosity on FF:** In the hydrodynamic regime, where sliding surfaces are separated by a full lubrication film, increasing viscosity will increase the FF. The oil film viscosity reduces with the increase of temperature, seriously affects the lubrication between ring and liner. Low viscosity multigrade oils reduce friction power losses, with a higher shear thinning effect than monograde oil. API CD, API CF, and API CF-4 are used to estimate viscosity's effect on FF between piston ring and cylinder liner. Oil viscosity depends on temperature, decreasing with higher temperatures. **Effect of Ring Tension on FF:** To obtain the effect of the ring tension, the Y Tateishi [18] model is used to calculate the FF. Higher ring tension leads to higher loading and again higher load ring decreases film thickness, and increases power loss and percentage of boundary lubrication. Figure 14 shows the FF is increased with increases the ring tension. For the lower ring tension of 150N the FF is minimum than that of higher ring tension according to the Y. Tateishi model.

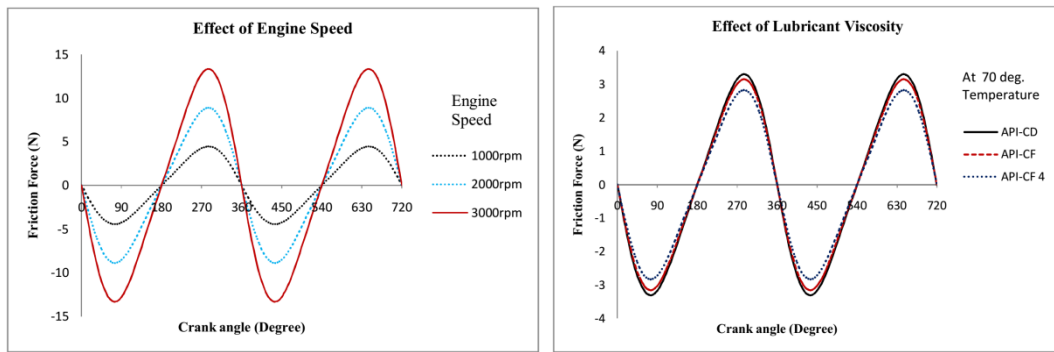


Fig. 13 Hydrodynamic Friction Force and Effect of Lubrication Viscosity at Different Engine Speed

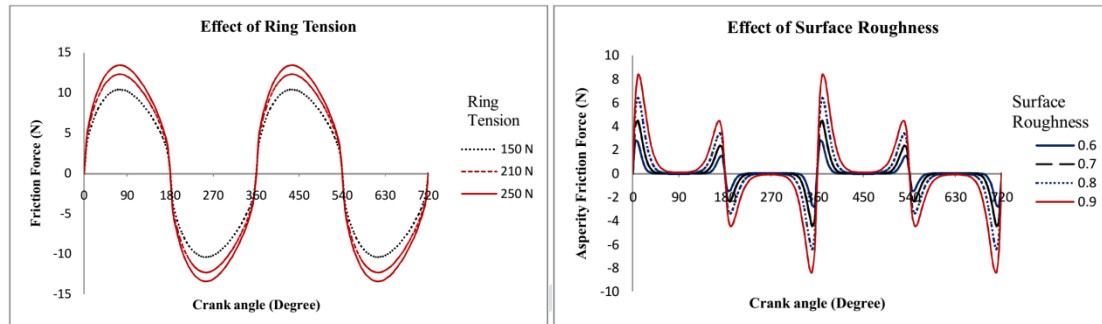


Fig. 14 Ring Tension on Friction Force and Asperity Friction Force for Different Surface Roughness

Effect of Surface Roughness on FF: The Akalin Newaz model reveals that FF increases with composite surface roughness of piston ring and cylinder liner, primarily due to asperity contact friction. The optimal surface roughness is 0.44 micron to minimize friction loss, but lower roughness results in metal to metal contact, increasing friction power loss. **Effect of Ring Width FF:** To know the effect of ring width on FF, Akalin Newaz [23] model is used where friction power loss is minimum at the minimum ring width and for the larger ring width, the FF is higher. Results shows that for 1.0mm ring width, the FF is 3.37N, for 1.5mm the FF is 5.30 N and for 2.0 mm the FF is about 6.5N. This is due to increase in contact surface of the ring with cylinder liner.

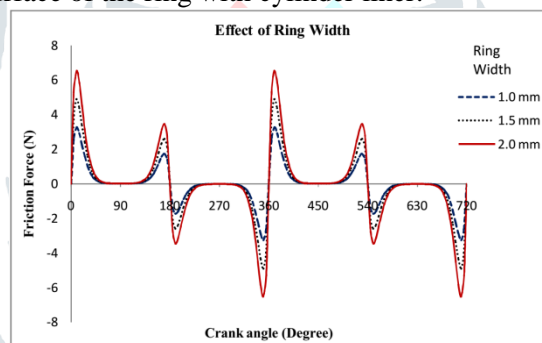


Fig.15 Effect of Ring Width on FF

VI. CONCLUSION AND FUTURE SCOPE

The piston ring assembly is culprit of major frictional power consumption in engine and hence tribological parameters of PRA are theoretically and experimentally analyzed through rotating disc test rig and on engine. The mechanical FF of the PRA is mainly depends upon the operating parameters like surface roughness of both piston ring and cylinder liner, piston velocity, lubricant viscosity, minimum oil film thickness, hydrodynamic pressure, asperity contact pressure and ring tension etc.

Experimental results of the kinematic viscosity of 03 lubricating oils with red wood viscometer were achieved and tabulated results are presented. It is found that all the lubricants show similar kind of pattern for viscosity v/s temperature performance. Further coating of piston ring was done with hard Chrome by electroplating and results for surface roughness were obtained. Smoother surfaces are found in second and third ring where as no change in surface roughness found after coating in first piston ring. It is also found that ring tension increases after coating of hard chrome. The choice of lubricant is important to reduce the FF on PRA as FF increases with increase ring width. The friction force of PRA also depends upon the surface roughness. The FF is maximum at the higher composite surface roughness.

Further, theoretical analysis based on few models were carried out for crank angle v/s piston velocity, minimum oil film thickness, hydrodynamic pressure and friction force, contact pressure and load, asperity friction force, and total friction load. It is found that the piston velocity is a significant parameter to decide the friction losses as piston velocity increases with increases engine speed, is highest at the mid of the stroke and smallest at the dead centers. OFT at the mid stroke of the engine cycle found to be most of large because of at that pure hydrodynamic lubrication

occurred. At the dead centers the thickness of oil film is very less because at that the piston velocity is low and due to oil squeeze effect. Hydrodynamic pressure is increases with increases the piston velocity with crank angle and nature of curved is found in sine wave. The hydrodynamic friction force found to be the maximum at the mid stroke of the engine cycle. The contact pressure depends on the OFT and it found higher at the TDC and BDC. The Contact pressure is lower at the centre position because there is a pure hydrodynamic lubrication occurrence. In addition, the contact load is also higher at the TDC and BDC and lower at the middle of the stroke. The asperity FF is maximum at the TDC and BDC but lower at the middle, stroke. It is observed that the total friction force is depends upon the both hydrodynamic as well as asperity friction force and is maximum about 7.7 N at dead centers.

Parametric analysis was carried out and it is found that the hydrodynamic friction force is maximum in case of 3000 rpm and concluded that the engine speed increases, the FF also increases. The API CD, API CF and API CF-4, are used to estimate the effect of viscosity on friction force between the piston ring and cylinder liner and found At the higher temperature the viscosity of the oil is get reduced in all conditions. It is found that higher ring tension leads to higher loading and again higher load ring decreases film thickness, and increases power loss and percentage of boundary lubrication. The asperity contact friction increases with the surface roughness due to the heavier surface asperity contact between rougher surfaces. It shows that the increase in the total ring pack friction is mainly contributed by asperity contact friction. As per final conclusion from the analysis, it is recommended to reduce the FF of the PRA by using the lubricants which maintain its characteristics at higher and lower temperatures. Preserve the composite surface roughness up to 0.44 micron for both ring and cylinder liner, because at that value the asperity friction force is minimum.

In conventional and coated ring, tests can be done with variability in load condition and sliding speed. Frictional force and frictional coefficient can be optimized in variable load and sliding conditions which may be a future scope of work.

REFERENCES

- [1] D. V Bhatt, "Simulation and Modeling of Friction Force and Oil Film Thickness in Piston Ring - Cylinder Liner Assembly of an I. C. Engine," *Lect. Notes Eng. Comput. Sci.*, vol. 2177, no. 1, 2009.
- [2] E. Abu-Nada, I. Al-Hinti, A. Al-Sarkhi, and B. Akash, "Effect of piston friction on the performance of SI engine: A new thermodynamic approach," *J. Eng. Gas Turbines Power*, vol. 130, no. 2, 2008, doi: 10.1115/1.2795777.
- [3] D. S. Joshi, A. V Shah, and D. C. Gosai, "Importance of Tribology in Internal Combustion Engine: A Review," *Int. Res. J. Eng. Technol.*, vol. 2, no. 7, 2015.
- [4] F. Zhu, J. Xu, X. Han, Y. Shen, and M. Jin, "Tribological performance of three surface-modified piston rings matched with chromium-plated cylinder liner," *Ind. Lubr. Tribol.*, vol. 69, no. 2, 2017, doi: 10.1108/ILT-11-2015-0164.
- [5] R. J. Gamble, M. Priest, and C. M. Taylor, "Detailed analysis of oil transport in the piston assembly of a gasoline engine," *Tribol. Lett.*, vol. 14, no. 2, 2003, doi: 10.1023/A:1021712506331.
- [6] M. Soejima, T. Hamatake, and Y. Harigaya, "Studies on Tribology to Reduce Friction, Wear and Lubricating Oil Consumption for Internal Combustion Engines," 2016.
- [7] D. V Bhatt, M. a Bulsara, and K. N. Mistry, "Prediction of oil film thickness in piston ring - cylinder assembly in an IC engine : a review," *World Congr. Eng.*, vol. II, 2009.
- [8] C. M. Taylor, "Automobile engine tribology-design considerations for efficiency and durability," *Wear*, vol. 221, no. 1, 1998, doi: 10.1016/S0043-1648(98)00253-1.
- [9] A. Kovalchenko, O. Ajayi, A. Erdemir, G. Fenske, and I. Etsion, "The effect of laser surface texturing on transitions in lubrication regimes during unidirectional sliding contact," in *Tribology International*, 2005, vol. 38, no. 3, doi: 10.1016/j.triboint.2004.08.004.
- [10] G. E. Totten, *Handbook of lubrication and tribology: Volume I application and maintenance, second edition*. 2006.
- [11] K. Wannatong, S. Chanchaona, and S. Sanitjai, "Simulation algorithm for piston ring dynamics," *Simul. Model. Pract. Theory*, vol. 16, no. 1, 2008, doi: 10.1016/j.simpat.2007.11.004.
- [12] C. Delprete and A. Razavykia, "Statistical Study of Ring Geometry Effect on Piston Ring/Liner Tribology Using Classical Design of Experiment," in *SAE Technical Papers*, 2018, vol. 2018-September, doi: 10.4271/2018-01-1658.
- [13] V. W. Wong and S. C. Tung, "Overview of automotive engine friction and reduction trends—Effects of surface, material, and lubricant-additive technologies," *Friction*, vol. 4, no. 1. 2016, doi: 10.1007/s40544-016-0107-9.
- [14] Z. Quan-bao, Z. Tie-zhu, and W. Rong-sheng, "A full lubrication model for rough surface piston rings," *Tribol. Int.*, vol. 21, no. 4, 1988, doi: 10.1016/0301-679X(88)90019-9.
- [15] Y. R. Jeng, "Theoretical analysis of piston-ring lubrication part i—fully flooded lubrication," *Tribol. Trans.*, vol. 35, no. 4, 1992, doi: 10.1080/10402009208982174.
- [16] Y. R. Jeng, "Theoretical analysis of piston-ring lubrication part ii—starved lubrication and its application to a complete ring pack," *Tribol. Trans.*, vol. 35, no. 4, 1992, doi: 10.1080/10402009208982175.
- [17] M. Gupta, S. Singhal, and S. Biswas, "Analytical investigation on the effect of multigrade oil in piston ring lubrication," *Tribol. Trans.*, vol. 37, no. 4, 1994, doi: 10.1080/10402009408983351.
- [18] Y. Tateishi, "Tribological issues in reducing piston ring friction losses," *Tribol. Int.*, vol. 27, no. 1, 1994, doi: 10.1016/0301-679X(94)90058-2.
- [19] "Two-dimensional piston ring lubrication - part I. rigid ring and liner solution," *Int. J. Multiph. Flow*, vol. 23, no. 7, 1997, doi: 10.1016/s0301-9322(97)80170-x.
- [20] Q. Yang and T. G. Keith, "Two-dimensional piston ring lubrication—part ii: elastic ring consideration," *Tribol. Trans.*, vol. 39, no. 4, 1996, doi: 10.1080/10402009608983607.
- [21] M. T. Ma, I. Sherrington, E. H. Smith, and N. Grice, "Development of a detailed model for piston-ring lubrication in IC

- engines with circular and non-circular cylinder bores,” *Tribol. Int.*, vol. 30, no. 11, 1997, doi: 10.1016/S0301-679X(97)00036-4.
- [22] D. E. Richardson, “Review of power cylinder friction for diesel engines,” *J. Eng. Gas Turbines Power*, vol. 122, no. 4, 2000, doi: 10.1115/1.1290592.
- [23] O. Akalin and G. M. Newaz, “Piston ring-cylinder bore friction modeling in mixed lubrication regime: Part I - Analytical results,” *J. Tribol.*, vol. 123, no. 1, 2001, doi: 10.1115/1.1286337.
- [24] O. Akalin and G. M. Newaz, “Piston ring-cylinder bore friction modeling in mixed lubrication regime: Part II - Correlation with bench test data,” *J. Tribol.*, vol. 123, no. 1, 2001, doi: 10.1115/1.1286338.
- [25] J. J. Truhan, J. Qu, and P. J. Blau, “A rig test to measure friction and wear of heavy duty diesel engine piston rings and cylinder liners using realistic lubricants,” in *Tribology International*, 2005, vol. 38, no. 3, doi: 10.1016/j.triboint.2004.08.003.
- [26] Z. Ma, N. A. Henein, and W. Bryzik, “A model for wear and friction in cylinder liners and piston rings,” *Tribol. Trans.*, vol. 49, no. 3, 2006, doi: 10.1080/05698190600678630.
- [27] Y. Harigaya, M. Suzuki, F. Toda, and M. Takiguchi, “Analysis of oil film thickness and heat transfer on a piston ring of a diesel engine: Effect of lubricant viscosity,” *J. Eng. Gas Turbines Power*, vol. 128, no. 3, 2006, doi: 10.1115/1.1924403.
- [28] E. Tomanik, “Friction and wear bench tests of different engine liner surface finishes,” *Tribol. Int.*, vol. 41, no. 11, 2008, doi: 10.1016/j.triboint.2007.11.019.
- [29] S. Johansson, P. H. Nilsson, R. Ohlsson, C. Anderberg, and B. G. Rosén, “New cylinder liner surfaces for low oil consumption,” *Tribol. Int.*, vol. 41, no. 9–10, 2008, doi: 10.1016/j.triboint.2008.02.012.
- [30] J. Williams, *Engineering tribology*, vol. 9780521609883. 2005.

